NEUTRON STAR MERGER

A radio counterpart to a neutron star merger

G. Hallinan,[1]*† A. Corsi,[2]† K. P. Mooley,[3] K. Hotokezaka,[4,5] E. Nakar,[6]
M. M. Kasliwal,[1] D. L. Kaplan,[7] D. A. Frail,[8] S. T. Myers,[8] T. Murphy,[9,10] K. De,[1]
D. Dobie,[9,10,11] J. R. Allison,[9,12] K. W. Bannister,[11] V. Bhalerao,[13] P. Chandra,[14]‡
T. E. Clarke,[15] S. Giacintucci,[15] A. Y. Q. Ho,[1] A. Horesh,[16] N. E. Kassim,[15]
S. R. Kulkarni,[1] E. Lenc,[9,10] F. J. Lockman,[17] C. Lynch,[9,10] D. Nichols,[18]
S. Nissanke,[18] N. Palliyaguru,[2] W. M. Peters,[15] T. Piran,[16] J. Rana,[19]
E. M. Sadler,[9,10] L. P. Singer[20]

Gravitational waves have been detected from a binary neutron star merger event, GW170817. The detection of electromagnetic radiation from the same source has shown that the merger occurred in the outskirts of the galaxy NGC 4993, at a distance of 40 megaparsecs from Earth. We report the detection of a counterpart radio source that appears 16 days after the event, allowing us to diagnose the energetics and environment of the merger. The observed radio emission can be explained by either a collimated ultrarelativistic jet, viewed off-axis, or a cocoon of mildly relativistic ejecta. Within 100 days of the merger, the radio light curves will enable observers to distinguish between these models, and the angular velocity and geometry of the debris will be directly measurable by very long baseline interferometry.

On 17 August 2017, the Advanced Laser Interferometer Gravitational Wave Observatory (Advanced LIGO) detected a gravitational wave signal, GW170817, which was rapidly identified to be associated with the inspiral and coalescence of two neutron stars (1). A burst of gamma rays, GRB 170817A, was detected approximately 2 s after the gravitational wave detection by the Gamma-ray Burst Monitor (GBM) of the Fermi Gamma-ray Space Telescope (2–4). With the addition of data from the Advanced Virgo interferometer, the source of gravitational waves was localized to an area of 28 deg^2 (90% confidence region) and a distance of 40 ± 8 Mpc (1). There were 49 cataloged galaxies within this volume, allowing astronomers to rapidly search for electromagnetic counterparts (5). An optical counterpart, designated SSS17a, was detected within ~11 hours of the event by astronomers using the Swope telescope, thereby localizing the merger to the S0-type galaxy NGC 4993 at a distance of 40 Mpc (6, 7); this was independently confirmed soon after (8, 9). After the optical detections, targeted observing campaigns were initiated across the electromagnetic spectrum (10). Subsequent optical and infrared spectroscopic obser-

vations firmly established this optical counterpart to be associated with the neutron star merger GW170817 (5).

We report a coordinated effort to use the Karl G. Jansky Very Large Array (VLA), the VLA Low Band Ionosphere and Transient Experiment (VLITE), the Australia Telescope Compact Array (ATCA), and the Giant Metrewave Radio Telescope (GMRT) to constrain the early-time radio properties of the neutron star merger. Companion papers report the ultraviolet and x-ray properties (11) and interpret the panchromatic behavior of the transient (5). The multiwavelength counterpart to GW170817 is hereafter referred to as EM170817.

The search for a radio counterpart to GW170817

We began radio observations of NGC 4993 on 17 August 2017 at 01:46 UTC, within ~13 hours of the detection of the gravitational event. These initial observations were part of a survey with the ATCA, targeting galaxies in the gravitational wave localization region as identified by the Census of the Local Universe (CLU) catalog (5). A similar survey of these CLU cataloged galaxies also commenced with the VLA. After confirma-

tion of a compelling optical counterpart to the merger, observations focused on the location of EM170817. Coordination among the VLA, ATCA, GMRT, and VLITE enabled monitoring on a near-daily basis at frequencies spanning 0.3 to 10 GHz (12). Only upper limits on the radio flux of EM170817 were possible until a counterpart appeared in VLA data from observations on 2 and 3 September 2017 at a frequency of 3 GHz, and in independent observations on 3 September at a frequency of 6 GHz (Fig. 1) (13, 14). The ATCA also detected the source on 5 September in the 5.5- to 9-GHz band (15). See table S1 for the entire radio data set. In observations at 3 GHz with the VLA, the source shows evidence of an increase in flux density over a time scale of 2 weeks, varying from 15.1 ± 3.9 μJy on 3 September to 34 ± 3.6 μJy on 17 September, where 1 Jy = 10^{-23} erg s^{-1} cm^{-2} Hz^{-1} (Figs. 2 and 3).

Figure 1 shows a comparison between a near-infrared image of EM170817 and deep radio images of the same field from the VLA at a frequency of 6 GHz. The position of the radio source is RA = 13h09m48.061s ± 0.005s, Dec = –23d22m53.35s ± 0.14s (J2000 equinox), using data at 3 GHz from 8 and 10 September 2017. The optical position derived from Hubble Space Telescope observations is RA = 13h09m48.071s ± 0.004s, Dec = –23d22m53.37s ± 0.05s (16). Within the uncertainties, the two positions are mutually consistent. We can further calculate the chance alignment of the optical counterpart to a background radio source. In these same radio data (8 and 10 September combined), the radio source has reached a flux density of 25 ± 2.2 μJy. There are 2700 sources per square degree with flux density greater or equal to this value at 3 GHz (17), resulting in a likelihood of chance alignment of 2 × 10^{-5} for the positional errors shown above. The likelihood of chance alignment becomes even smaller when considering that the source has been observed to double in flux density over 2 weeks and that fewer than 4% of sources at 3 GHz vary by >30% (18). We therefore confirm the transient to be the radio counterpart to EM170817.

Models of binary neutron star coalescence predict the emergence of an associated radio flare due to the tidal ejection of 0.01 to 0.05 solar masses ($M_\odot$) of energetic material at subrelativistic velocities (a few tenths of the speed of light) (19–21). This ejecta material forms a blast wave as it plows through the ambient interstellar medium (ISM) surrounding the merger,

[1]Division of Physics, Mathematics and Astronomy, California Institute of Technology, Pasadena, CA 91125, USA. [2]Department of Physics and Astronomy, Texas Tech University, Lubbock, TX 79409, USA. [3]Astrophysics, Department of Physics, University of Oxford, Oxford OX1 3RH, UK. [4]Center for Computational Astrophysics, Flatiron Institute, 162 5th Avenue, New York, NY 10010, USA. [5]Department of Astrophysical Sciences, Princeton University, Princeton, NJ 08544, USA. [6]Raymond and Beverly Sackler School of Physics and Astronomy, Tel Aviv University, Tel Aviv 69978, Israel. [7]Department of Physics, University of Wisconsin, Milwaukee, WI 53201, USA. [8]National Radio Astronomy Observatory, Socorro, NM 87801, USA. [9]Sydney Institute for Astronomy, School of Physics, University of Sydney, Sydney, NSW 2006, Australia. [10]Australian Research Council Centre of Excellence for All-sky Astrophysics (CAASTRO). [11]Australia Telescope National Facility, Commonwealth Scientific and Industrial Research Organisation, Astronomy and Space Science, Epping, NSW 1710, Australia. [12]Australian Research Council Centre of Excellence for All-sky Astrophysics in 3 Dimensions (ASTRO 3D). [13]Department of Physics, Indian Institute of Technology Bombay, Mumbai 400076, India. [14]National Centre for Radio Astrophysics, Tata Institute of Fundamental Research, Pune University Campus, Ganeshkhind Pune 411007, India. [15]Remote Sensing Division, Naval Research Laboratory, Washington, DC 20375, USA. [16]Racah Institute of Physics, Hebrew University of Jerusalem, Jerusalem 91904, Israel. [17]Green Bank Observatory, Green Bank, WV 24944, USA. [18]Institute of Mathematics, Astrophysics and Particle Physics, Radboud University, 6525 AJ Nijmegen, Netherlands. [19]Inter University Centre for Astronomy and Astrophysics, Pune University Campus, Pune, Maharashtra 411007, India. [20]Astroparticle Physics Laboratory, NASA Goddard Space Flight Center, Greenbelt, MD 20771, USA.
*Corresponding author. Email: gh@astro.caltech.edu †These authors contributed equally to this work. ‡Present address: Department of Astronomy, Stockholm University, Alba Nova, SE-106 91 Stockholm, Sweden.

producing synchrotron radiation peaking at radio frequencies, lasting months to years after the merger. The observed time scale and luminosity of the radio source are sensitive to the mass and velocity of the blast wave ejecta and the density of the ISM. Therefore, the radio emission is diagnostic of the energetics of the blast wave ejecta as well as the environment of the merger.

Binary neutron star mergers have long been proposed as a likely progenitor for short (<2 s) hard gamma-ray bursts (sGRBs) (22), and the generation of an ultrarelativistic jet is required to account for the properties of both the GRBs and their afterglows (23). As in the case of subrelativistic ejecta, the jet interacting with the circum-merger medium will produce radio emission. However, in this case, the resulting radio light curve depends critically on the angle between the observer line of sight and the jet (24).

We compare our early-time radio observations with numerical models (12) for the expected radio light curves attributable to synchrotron emission from subrelativistic ejecta and an ultrarelativistic jet, as well as the interaction between these components. Where possible, we focus on a portion of the parameter space that is consistent with observations at x-ray wavelengths [see figure 5 of (5) for a schematic illustration of the model].

The subrelativistic ejecta

The radio flare produced by the subrelativistic ejecta that generates the optical and infrared emission is expected to peak on a time scale of months to years (19–21). With the mass and velocity range inferred from the optical and infrared, its energy must be high (>10^{51} erg) (5); however, with an expected velocity of ~$0.2c$, the bulk of this ejecta cannot be the

source of the radio signal that has been observed to rise within weeks of the merger. Instead, this component is expected to dominate the radio emission at late time (years). Nonetheless, this ejecta is expected to have a distribution of velocities with a low-mass fast tail that can extend up to mildly relativistic velocities, which may be the source of the observed emission (Fig. 3). When considering the subrelativistic ejecta, we take into account the nondetection of neutral hydrogen from the host galaxy (5σ mass limit of <$1 \times 10^8 M_\odot$) in our recent observations with the Green Bank Telescope [GBT (12)], which suggests an ISM density $n < 0.04$ cm^{-3} (see supplementary text). Assuming this density to be a constraining limit, the radio then requires such a mildly relativistic outflow to have a velocity $v > 0.7c$ (Lorentz factor $\Gamma > 1.4$) and to carry at least 10^{49} erg in isotropic equivalent energy (Fig. 3). This is unlikely but cannot be ruled out.

### A classical short hard gamma-ray burst

GW170817 provides an unambiguous detection of a binary neutron star merger and therefore offers the opportunity to directly investigate the presence of an ultrarelativistic jet. The isotropic equivalent luminosity of the burst of gamma rays detected by the Fermi GBM is 4×10^{46} erg (2–4). This is orders of magnitude lower than the peak luminosity of the classical sGRB population (10^{49} to 10^{52} erg; median = 2×10^{51} erg) (23). Moreover, this gamma-ray emission is not a very-low-luminosity analog of the classical sGRB population (5).

Therefore, the observed gamma rays cannot securely confirm the long-standing hypothesis that neutron star mergers are the progenitors of cosmological sGRBs. Within the framework of the classical short hard GRB

model, there are two possibilities: (i) The jet axis was slightly offset from our line of sight but was close enough for the observed gamma rays to be a component of the regular sGRB prompt emission (hereafter called the slightly off-axis model); or (ii) our line of sight was at a large angle from the jet axis, and the observed gamma rays were generated by a different mechanism (hereafter called the widely off-axis model). Below, we explore the current radio constraints and predict the future evolution under each of these scenarios.

In the slightly off-axis model, if the gamma rays are produced by a slightly off-axis jet, then the edge of the jet cannot be more than about 0.1 rad from our line of sight (5). The jet drives a relativistic blast wave into the ISM, which subsequently decelerates quickly. The Lorentz factor Γ drops to ~10 within about a day, after which the beam of its emission expands to include our line of sight, thereby producing bright radio emission in our direction. The blast wave Lorentz factor at a given time depends very weakly on the jet isotropic equivalent energy E_{iso} and the external number density n; therefore, this prediction holds for a wide range of jet and ISM parameters (25).

Figure 2 shows several predicted light curves (12) for an ultrarelativistic jet with $E_{iso} = 10^{50}$ erg that misses our line of sight by 0.1 rad. A density of 10^{-3} cm^{-3}, which is on the low end of the distribution of densities inferred from sGRB afterglows (26), produces a signal that is brighter than the observed radio emission from EM170817 by more than an order of magnitude. A very low density of 6×10^{-7} cm^{-3} is required to reproduce the observed light curve, which is more consistent with the intergalactic medium than with the environs of an S0-type galaxy (27). Therefore, our radio observations strongly
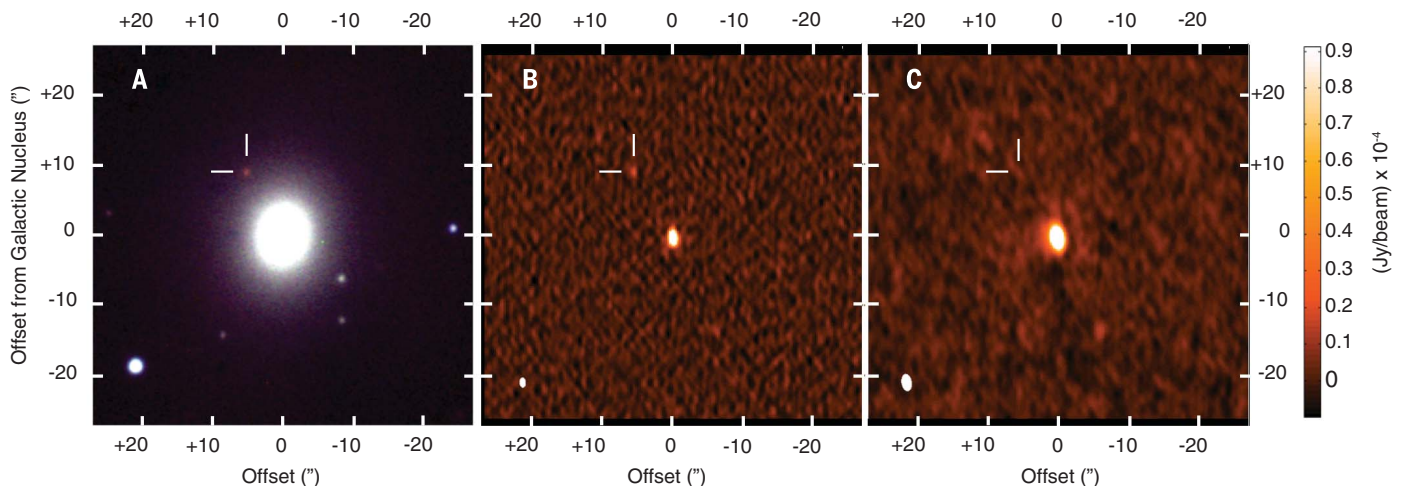
Fig. 1. Comparison of the near-infrared and radio counterparts to EM170817. (**A**) Near-infrared image of NGC 4993 with EM170817 highlighted, assembled from *J*, *H*, and *Ks* photometric bands taken with the FLAMINGOS-2 instrument on Gemini-South on 27 August 2017 (3). (**B**) Radio image of the same field created using VLA observations (6 GHz) on 9 September 2017, with the radio counterpart to EM170817

highlighted. Its flux density is 23 ± 3.4 μJy. (**C**) A combined image from four VLA observations at 6 GHz spanning 22.6 August to 1 September 2017. The flux density at the position of EM170817 is 7.8 ± 2.6 μJy, consistent with a marginal detection or nondetection. Radio emission seen in (B) and (C) from the core of the galaxy is due to an active galactic nucleus.

disfavor a model in which the observed gamma rays were produced by a slightly off-axis luminous ultrarelativistic jet.

Under the widely off-axis model, the radio data are consistent with the model for reasonable ranges of jet energy and ISM density (Fig. 3). The radio emission from an off-axis jet undergoes a rapid rise before a broad peak, followed by a slow decline. The observed radio light curve of EM170817 is inconsistent with the sharp rise phase of an off-axis jet. Instead, the light curve implies that the observations were made around the onset of the broad peak in emission. Thus, a prediction of this model is that the radio light curve will remain at a similar brightness for the next several weeks and then start to fade. However, this model does not account for the early-time gamma-ray emission.

A mildly relativistic cocoon

The high luminosity of the optical and infrared counterpart to EM170817 requires a high mass of ejecta at subrelativistic velocities at the time of the merger (5). The observed delay between the gravitational wave signal of the neutron star merger and the Fermi-detected gamma rays indicates an additional sustained source of energy after the merger. This source of energy is likely manifested as a jet. As it expands, the jet transfers a large fraction of its energy into the surrounding ejecta, forming a hot cocoon that expands over a wide angle while traveling at mildly relativistic velocities (28). The formation and possible eventual breakout of such a cocoon can account for many of the properties of the observed electromagnetic signatures seen after the event, from infrared to gamma rays (5). As this cocoon propagates into the ISM, it will also produce a radio signal.

The energy coupled to the mildly relativistic ejecta depends mostly on the fate of the jet as well as its total energy. If the jet is narrow (opening angle ~10°), it can drill through the ejecta and break out with an isotropic equivalent energy of ~10^{50} to 10^{51} erg, leaving a fraction of its total energy (10^{48} to 10^{49} erg) in the mildly relativistic cocoon. Alternatively, if the jet is wide, it requires about 10^{51} erg in order to propagate a substantial distance within the ejecta before it is fully choked, depositing all of its energy in the cocoon. A non-negligible fraction of this energy, >10^{50} erg, is then coupled to mildly relativistic ejecta with $\Gamma = 2$ to 3 (and possibly even higher). Thus, an energetic, mildly relativistic outflow indicates a choked jet, whereas a low-energy, mildly relativistic outflow indicates a narrow jet that breaks out of the ejecta.

Figure 3 shows the predicted radio emission for both scenarios (12), assuming $\Gamma = 2$; both are consistent with the observed radio emission if the ISM density is about ~3×10^{-3} cm^{-3} ($\Gamma = 3$ requires a density of ~3×10^{-4} cm^{-3}). Both curves are similar during the rising phase, as the radio emission is generated by the forward shock propagating into the ISM with luminosity
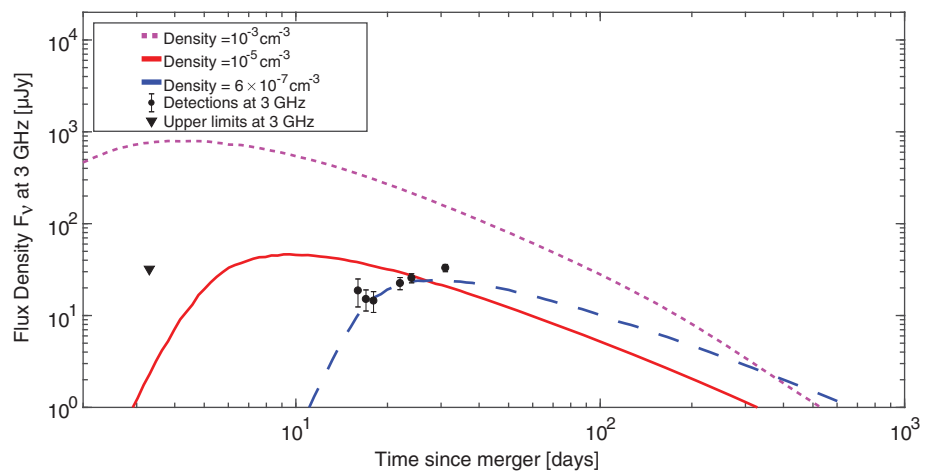
Fig. 2. Radio observations rule out a slightly off-axis jet. Invoking a slightly off-axis jet to explain the Fermi-detected gamma rays from EM170817 (3) would require an associated radio afterglow appearing within a few days. The radio counterpart to EM170817 is inconsistent with this model. Light curves are shown for three examples, each with a jet isotropic equivalent energy $E_{iso} = 10^{50}$ erg, a jet half-opening angle of ~25°, and an angle between our line of sight and the jet of ~30°. The only parameter that varies among them is density. The light curves associated with a density of 10^{-3} cm^{-3} (pink dotted curve) and 10^{-5} cm^{-3} (red solid curve) are completely inconsistent with the data. The data can be fitted by a model of a jet ($E_{iso} = 4 \times 10^{50}$ erg) interacting with an ISM density of 6×10^{-7} cm^{-3} (blue dashed curve), which is inconsistent with the ISM density of a galaxy.
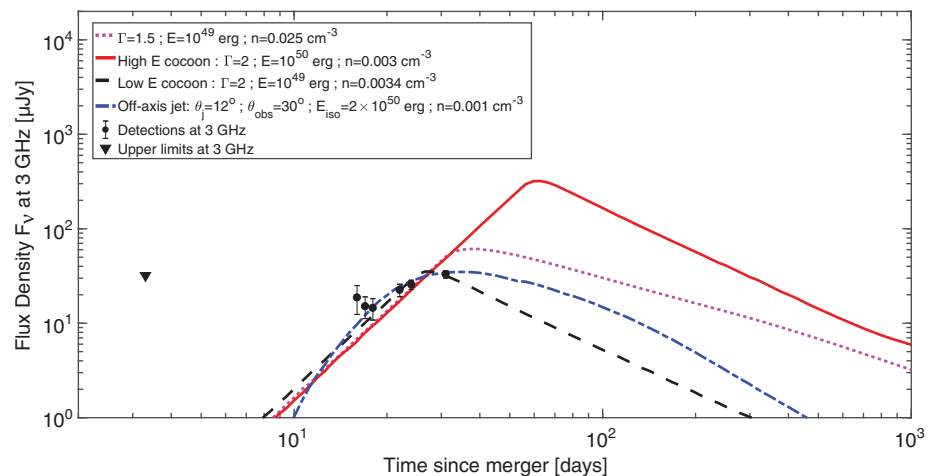
Fig. 3. Radio light curve is consistent with either an off-axis jet or a cocoon. Light curves are shown for both proposed cocoon models: a high-energy cocoon attributable to a choked jet (red solid curve) and a low-energy cocoon with jet breakout (black dashed curve). The light curve favors the low-energy cocoon with jet breakout. For the off-axis jet, we use a jet isotropic equivalent energy $E_{iso} = 1.5 \times 10^{50}$ erg, a jet half-opening angle $\theta_j \approx 12°$, and an angle between our line of sight and the jet $\theta_{obs} \sim 30°$, together with an ISM density of 10^{-3} cm^{-3} (blue dash-dot curve). However, the light curve is consistent with a range of parameter space in jet energy and ISM density. For each set of jet and observer angle, there is a single solution (namely n and E) that fit the data, which cannot be distinguished from the light curve. The pink dotted curve is a model that represents the expected radio emission attributable to the high-velocity tail of the subrelativistic ejecta, which is yet to be ruled out. All the models indicate an ISM density of ~10^{-3} to 10^{-2} cm^{-3}, which in turn is consistent with constraints from H I upper limits (supplementary text). We predict that within the first 100 days of the merger, the radio light curves will enable one of these models to be distinguished.
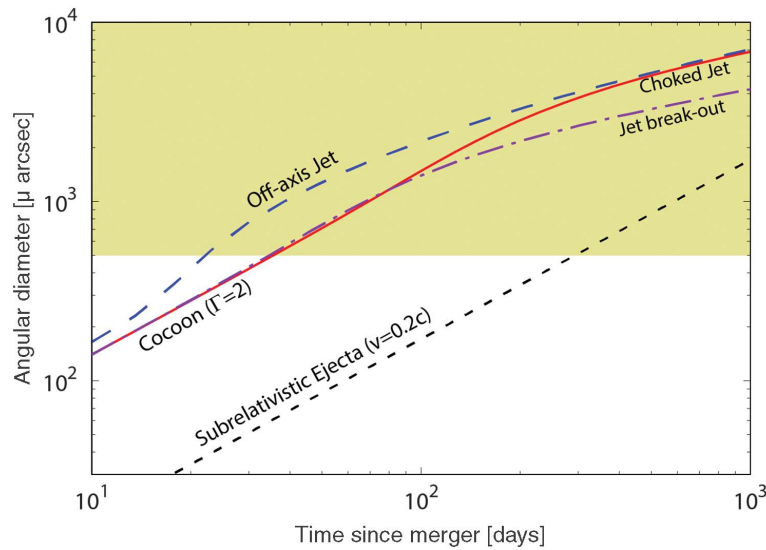
Fig. 4. Predicted time evolution of the radio source size for different models. Different possible models for the radio emission from EM170817 expand at different velocities. The yellow area shows the approximate parameter space accessible to VLBI. Model parameters for the off-axis jet and cocoon models are the same as used in Fig. 3. The subrelativistic ejecta is assumed to have a bulk velocity of 0.2c (see text). We note that this represents a conservative lower limit to the source size, as the radio emission is dominated by the fastest component of the ejecta (which can exceed 0.4c).

that depends only on velocity (for a given density). This velocity is constant during the rising phase. During this phase, the radio flux at a given band rises as time t^3 over a wide range of parameters, regardless of the shock velocity (whether Newtonian or relativistic), cocoon energy, or ISM density. The emission peaks when the entire energy of the cocoon is deposited in the ISM and the shock starts to decelerate. Thus, an energetic cocoon may become much brighter several months after a merger, whereas a low-energy cocoon persists for much less time. The current data marginally favor the low-energy cocoon model (jet breakout) over the energetic cocoon (choked jet). We predict that the radio light curves will definitively allow us to discriminate among an energetic cocoon, a low-energy cocoon, and an off-axis jet model within 100 days of the merger.

Consistency with the x-ray observations

All the models that we have considered predict an optically thin spectrum, consistent with our radio observations (fig. S4), with a single power law between the radio and the x-rays, $F_\nu \propto \nu^{-\beta}$, where F_ν is flux density, ν is frequency, and β is the spectral power-law index; in turn, β depends on the electron distribution power-law index, p, as $\beta = (p − 1)/2$. Thus, all our models predict the same x-ray flux around the time that the radio emission was detected. This flux is broadly consistent with the x-ray measurement at 15 days (29, 30) if $\beta = 0.5$ ($p = 2$). This spectral index and value of p are lower than typically observed in GRB afterglows, although there are afterglows where

such values are measured (31). If $p > 2$, then the models of the radio emission predict an x-ray flux that is lower than the observed one. In that case, the observed x-rays must not be produced by the blast wave that propagates into the ISM, but by some other source.

Imaging the fireball of GW170817

Our models predict differing sizes for the expanding radio-emission region (Fig. 4). Radio observations can directly and indirectly constrain the size of the expanding fireball, as has been demonstrated in the case of long GRBs (32, 33).

Radio sources of compact size can be observed to vary, sometimes by a large degree on short time scales, as a result of interstellar scintillation due to propagation through the ISM of our own Galaxy. This variability, analogous to the twinkling of compact objects observed at optical wavelengths, can be used to indirectly measure the size of compact radio sources (34). Using a simple model of the ISM in our Galaxy, inferred from observations of pulsars (35), we predict that the radio counterpart to EM170817 will be subject to refractive scintillation in the strong scattering regime. In fig. S5, we calculate the expected modulation index and characteristic time scale for scintillation of the various possible components of ejecta; we find the degree of modulation unlikely to be useful in constraining the source size, given the low signal-to-noise ratio of the radio detections, except in the case of subrelativistic ejecta. Conversely, this suggests that the light curves presented in Figs. 2 and 3 are reliable measures of the

intrinsic variability of EM170817, not misidentified scintillation.

A more direct method to constrain the size of the afterglow and directly measure the outflow front velocity is very long baseline interferometry (VLBI), which has been successfully applied to the case of long GRBs (33). We predict that EM170817 will become detectable and resolved on VLBI baselines within 100 days of the merger, providing an independent constraint on the nature of the ejecta (Fig. 4).

REFERENCES AND NOTES

1. LIGO Scientific Collaboration and Virgo Collaboration, *Phys. Rev. Lett.* **119**, 161101 (2017).
2. A. Goldstein *et al.*, *Gamma Ray Coordinates Network Circular 21528* (2017).
3. B. P. Abbott *et al.*, *Astrophys. J.* 10.3847/2041-8213/aa920c (2017).
4. A. Goldstein *et al.*, *Astrophys. J.* 10.3847/2041-8213/aa8f41 (2017).
5. M. M. Kasliwal *et al.*, *Science* **358**, 1559–1565 (2017).
6. D. Coulter *et al.*, *Gamma Ray Coordinates Network Circular 21529* (2017).
7. D. A. Coulter *et al.*, *Science* **358**, 1556–1558 (2017).
8. S. Allam *et al.*, *Gamma Ray Coordinates Network Circular 21530* (2017).
9. S. Yang *et al.*, *Gamma Ray Coordinates Network Circular 21531* (2017).
10. B. Abbott *et al.*, *Astrophys. J.* 10.3847/2041-8213/aa91c9 (2017).
11. P. A. Evans *et al.*, *Science* **358**, 1565–1570 (2017).
12. See supplementary materials.
13. K. Mooley, G. Hallinan, A. Corsi, *Gamma Ray Coordinates Network Circular 21814* (2017).
14. A. Corsi, G. Hallinan, K. Mooley, *Gamma Ray Coordinates Network Circular 21815* (2017).
15. T. Murphy *et al.*, *Gamma Ray Coordinates Network Circular 21842* (2017).
16. S. M. Adams, M. M. Kasliwal, N. Blagorodnova, *Gamma Ray Coordinates Network Circular 21816* (2017).
17. V. Smolčić *et al.*, *Astron. Astrophys.* **602**, A1 (2017).
18. K. P. Mooley *et al.*, *Astrophys. J.* **818**, 105 (2016).
19. E. Nakar, T. Piran, *Nature* **478**, 82–84 (2011).
20. K. Hotokezaka, T. Piran, *Mon. Not. R. Astron. Soc.* **450**, 1430–1440 (2015).
21. K. Hotokezaka *et al.*, *Astrophys. J.* **831**, 190 (2016).
22. D. Eichler, M. Livio, T. Piran, D. N. Schramm, *Nature* **340**, 126–128 (1989).
23. E. Nakar, *Phys. Rep.* **442**, 166–236 (2007).
24. J. Granot, A. Panaitescu, P. Kumar, S. E. Woosley, *Astrophys. J.* **570**, L61–L64 (2002).
25. R. Sari, T. Piran, R. Narayan, *Astrophys. J.* **497**, L17–L20 (1998).
26. E. Berger, *Annu. Rev. Astron. Astrophys.* **52**, 43–105 (2014).
27. P. Serra *et al.*, *Mon. Not. R. Astron. Soc.* **422**, 1835–1862 (2012).
28. O. Gottlieb, E. Nakar, T. Piran, arXiv:1705.10797. (2017).
29. E. Troja *et al.*, *Gamma Ray Coordinates Network Circular 21765* (2017).
30. E. Troja *et al.*, *Nature* 10.1038/nature24290 (2017).
31. X.-G. Wang *et al.*, *Astrophys. J. Suppl. Ser.* **219**, 9 (2015).
32. S. R. Kulkarni *et al.*, *Nature* **395**, 663–669 (1998).
33. G. B. Taylor, D. A. Frail, E. Berger, S. R. Kulkarni, *Astrophys. J.* **609**, L1–L4 (2004).
34. M. A. Walker, *Mon. Not. R. Astron. Soc.* **294**, 307–311 (1998).

35. J. M. Cordes, T. J. W. Lazio, arXiv:astro-ph/0207156 (2002).

SUPPLEMENTARY MATERIALS

www.sciencemag.org/content/358/6370/1579/suppl/DC1
Materials and Methods
Supplementary Text
Figs. S1 to S5
Table S1
References (36–65)

17 September 2017; accepted 9 October 2017
Published online 16 October 2017
10.1126/science.aap9855

Science

A radio counterpart to a neutron star merger

G. Hallinan, A. Corsi, K. P. Mooley, K. Hotokezaka, E. Nakar, M. M. Kasliwal, D. L. Kaplan, D. A. Frail, S. T. Myers, T. Murphy, K. De, D. Dobie, J. R. Allison, K. W. Bannister, V. Bhalerao, P. Chandra, T. E. Clarke, S. Giacintucci, A. Y. Q. Ho, A. Horesh, N. E. Kassim, S. R. Kulkarni, E. Lenc, F. J. Lockman, C. Lynch, D. Nichols, S. Nissanke, N. Palliyaguru, W. M. Peters, T. Piran, J. Rana, E. M. Sadler and L. P. Singer

GROWTH observations of GW170817

The gravitational wave event GW170817 was caused by the merger of two neutron stars (see the Introduction by Smith). In three papers, teams associated with the GROWTH (Global Relay of Observatories Watching Transients Happen) project present their observations of the event at wavelengths from x-rays to radio waves. Evans *et al.* used space telescopes to detect GW170817 in the ultraviolet and place limits on its x-ray flux, showing that the merger generated a hot explosion known as a blue kilonova. Hallinan *et al.* describe radio emissions generated as the explosion slammed into the surrounding gas within the host galaxy. Kasliwal *et al.* present additional observations in the optical and infrared and formulate a model for the event involving a cocoon of material expanding at close to the speed of light, matching the data at all observed wavelengths.
Science, this issue p. 1565, p. 1579, p. 1559; see also p. 1554

ARTICLE TOOLS	http://science.sciencemag.org/content/358/6370/1579
SUPPLEMENTARY MATERIALS	http://science.sciencemag.org/content/suppl/2017/10/13/science.aap9855.DC1
RELATED CONTENT	file:/content
	http://science.sciencemag.org/content/sci/358/6370/1556.full
	http://science.sciencemag.org/content/sci/358/6370/1570.full
	http://science.sciencemag.org/content/sci/358/6370/1574.full
	http://science.sciencemag.org/content/sci/358/6361/301.full
	http://science.sciencemag.org/content/sci/358/6370/1565.full
	http://science.sciencemag.org/content/sci/358/6370/1559.full
	http://science.sciencemag.org/content/sci/358/6370/1583.full
	http://science.sciencemag.org/content/sci/358/6370/1554.full
	http://science.sciencemag.org/content/sci/358/6370/1504.full
REFERENCES	This article cites 36 articles, 3 of which you can access for free
	http://science.sciencemag.org/content/358/6370/1579#BIBL